

TUBERCULOSIS

Rapid detection of *Mycobacterium tuberculosis* in sputum with a solvatochromic trehalose probe

Mireille Kamariza,^{1*} Peyton Shieh,^{2*} Christopher S. Ealand,³ Julian S. Peters,³ Brian Chu,² Frances P. Rodriguez-Rivera,² Mohammed R. Babu Sait,⁴ William V. Treuren,⁵ Neil Martinson,^{3,6} Rainer Kalscheuer,⁴ Bavesh D. Kana,^{3,7} Carolyn R. Bertozzi^{2,8†}

Copyright © 2018
The Authors, some
rights reserved;
exclusive licensee
American Association
for the Advancement
of Science. No claim
to original U.S.
Government Works

Tuberculosis (TB) is the leading cause of death from an infectious bacterial disease. Poor diagnostic tools to detect active disease plague TB control programs and affect patient care. Accurate detection of live *Mycobacterium tuberculosis* (Mtb), the causative agent of TB, could improve TB diagnosis and patient treatment. We report that mycobacteria and other corynebacteria can be specifically detected with a fluorogenic trehalose analog. We designed a 4-*N,N*-dimethylamino-1,8-naphthalimide-conjugated trehalose (DMN-Tre) probe that undergoes >700-fold increase in fluorescence intensity when transitioned from aqueous to hydrophobic environments. This enhancement occurs upon metabolic conversion of DMN-Tre to trehalose monomycolate and incorporation into the mycomembrane of Actinobacteria. DMN-Tre labeling enabled the rapid, no-wash visualization of mycobacterial and corynebacterial species without nonspecific labeling of Gram-positive or Gram-negative bacteria. DMN-Tre labeling was detected within minutes and was inhibited by heat killing of mycobacteria. Furthermore, DMN-Tre labeling was reduced by treatment with TB drugs, unlike the clinically used auramine stain. Lastly, DMN-Tre labeled Mtb in TB-positive human sputum samples comparably to auramine staining, suggesting that this operationally simple method may be deployable for TB diagnosis.

INTRODUCTION

Tuberculosis (TB), caused by *Mycobacterium tuberculosis* (Mtb), is a serious global health challenge causing an estimated 1.8 million deaths in 2015 (1). The increasing number of Mtb strains resistant to courses of treatment has exacerbated the global epidemic (2–4). The standard approach for rapid TB diagnosis in high-burden geographic areas is the detection of Mtb in sputum or extrapulmonary sites using the color-based Ziehl-Neelsen (ZN) test, developed more than 100 years ago (5–7), or the fluorescent auramine-based Truant stain, first reported in 1938 (8). Both tests rely on the propensity of the mycobacterial outer membrane, also called the mycomembrane, to bind and retain hydrophobic dyes (9, 10). The staining protocols require extensive processing to remove excess dye from debris and other bacteria, whereas the dye must be retained by mycobacteria. Thus, the sensitivity of these tests varies widely (32 to 94%) depending on the method used and on the experience of the user (11, 12). In addition, current diagnostic tests cannot distinguish live from dead or drug-compromised mycobacteria (2) and, therefore, cannot report on treatment efficacy or guide clinical decision-making in the face of rising drug resistance. New tools to advance sputum-based diagnostic accuracy, simplicity, and specificity for viable organisms are urgently needed.

In the century since the ZN and Truant staining methods were developed, much has been learned about the molecular composition of the mycomembrane (13). Trehalose-based glycolipids are major components, most prominently trehalose mono- and dimycolates, and are known to be essential for Mtb cell viability (14, 15). Trehalose mycolates are thought to be unique to the Actinobacteria phylum, which includes pathogenic mycobacteria and corynebacteria but not canonical Gram-positive or Gram-negative organisms nor human hosts. Therefore, a staining method that targets trehalose mycolates may improve the specificity of Mtb detection in sputum samples.

Several groups, including ours, have observed that modified trehalose analogs, including fluorine- (16, 17), azide- (18), alkyne- (19), or fluorophore-functionalized derivatives (16, 20), can be metabolically incorporated into the mycobacterial outer membrane as trehalose mycolates. Indeed, fluorinated trehalose analogs have potential application for positron emission tomography imaging of lung-resident Mtb (17, 21). Metabolic processing is enabled by the substrate promiscuity of the antigen 85 (Ag85) complex that catalyzes mycolylation of trehalose (22). This enzyme system permits chemical modification at specific sites of one of the glucose moieties, including the addition of a fluorophore whose mass exceeds that of the underlying disaccharide, without catastrophic loss of enzymatic conversion. Because the process depends on active metabolism, Mtb labeling with trehalose analogs might distinguish viable from dead or drug-compromised bacteria, a capability lacking in current Mtb staining methods. Accordingly, we considered the possible use of fluorescent trehalose analogs for the detection of viable Mtb in sputum samples, but the necessity of removing unmetabolized probe to eliminate background fluorescence proved to be a major impediment. A trehalose probe whose fluorescence signal is specifically activated by metabolic incorporation into the mycomembrane would overcome such a limitation.

Here, we show that trehalose conjugated to the solvatochromic dye 4-*N,N*-dimethylamino-1,8-naphthalimide (DMN), a reagent we termed DMN-Tre, is metabolically incorporated into mycomembranes

¹Department of Biology, Stanford University, Stanford, CA 94305, USA. ²Department of Chemistry, Stanford University, Stanford, CA 94305, USA. ³Department of Science and Technology/National Research Foundation Centre of Excellence for Biomedical Tuberculosis Research, Faculty of Health Sciences, University of Witwatersrand, National Health Laboratory Service, Johannesburg, South Africa. ⁴Institute of Pharmaceutical Biology and Biotechnology, Heinrich Heine University Duesseldorf, Universitätsstrasse 1, 40225 Duesseldorf, Germany. ⁵Department of Microbiology and Immunology, Stanford University, Stanford, CA 94305, USA. ⁶Perinatal HIV Research Unit (PHRU), SA MRC Soweto Matlosana Collaborating Centre for HIV/AIDS and TB, University of the Witwatersrand, Johannesburg, South Africa. ⁷Medical Research Council—Centre for the AIDS Programme of Research in South Africa (CAPRISA) HIV-TB Pathogenesis and Treatment Research Unit, Durban, South Africa. ⁸Howard Hughes Medical Institute, Stanford University, Stanford, CA 94305, USA.

*These authors contributed equally to this work.

†Corresponding author. Email: bertozzi@stanford.edu

where it undergoes a marked enhancement in fluorescence that enables the detection of mycobacteria in sputum samples from patients with TB in under an hour. Unlike the classic ZN and auramine stains, DMN-Tre labeling is diminished by exposure to front-line TB drugs, reflecting their influence on cell viability. This operationally simple labeling method requires a single incubation step without washes and may therefore powerfully complement current methods for TB diagnosis at the point of care.

RESULTS

Trehalose mycolates are unique to the Actinobacteria phylum

Trehalose dye conjugates can be metabolically incorporated into the mycobacterial outer membrane as trehalose mycolates (Fig. 1A). To evaluate the specificity of this method, we performed a tblastn anal-

ysis of the National Center for Biotechnology Information bacterial database in search of acyl transferase Ag85 protein complex homologs [the enzymes responsible for mycolylation of trehalose (22)] and found that they were largely restricted to the Actinomycetales order (Fig. 1, B and C, and table S1). In contrast, the most abundant constituents of the lung microbiome [such as members of the Proteobacteria, Firmicutes, and Bacteroidetes phyla and the *Pseudomonas*, *Streptococcus*, *Prevotella*, *Fusobacterium*, and *Veillonella* genera (23, 24)] do not have identifiable Ag85 homologs.

An environment-sensitive fluorogenic trehalose probe permits the fast, specific no-wash detection of mycobacteria and corynebacteria

We chose the environmentally sensitive DMN dye based on the observation of Imperiali and co-workers (25–27) that the molecule exhibits a marked fluorescence when transitioned from aqueous to organic

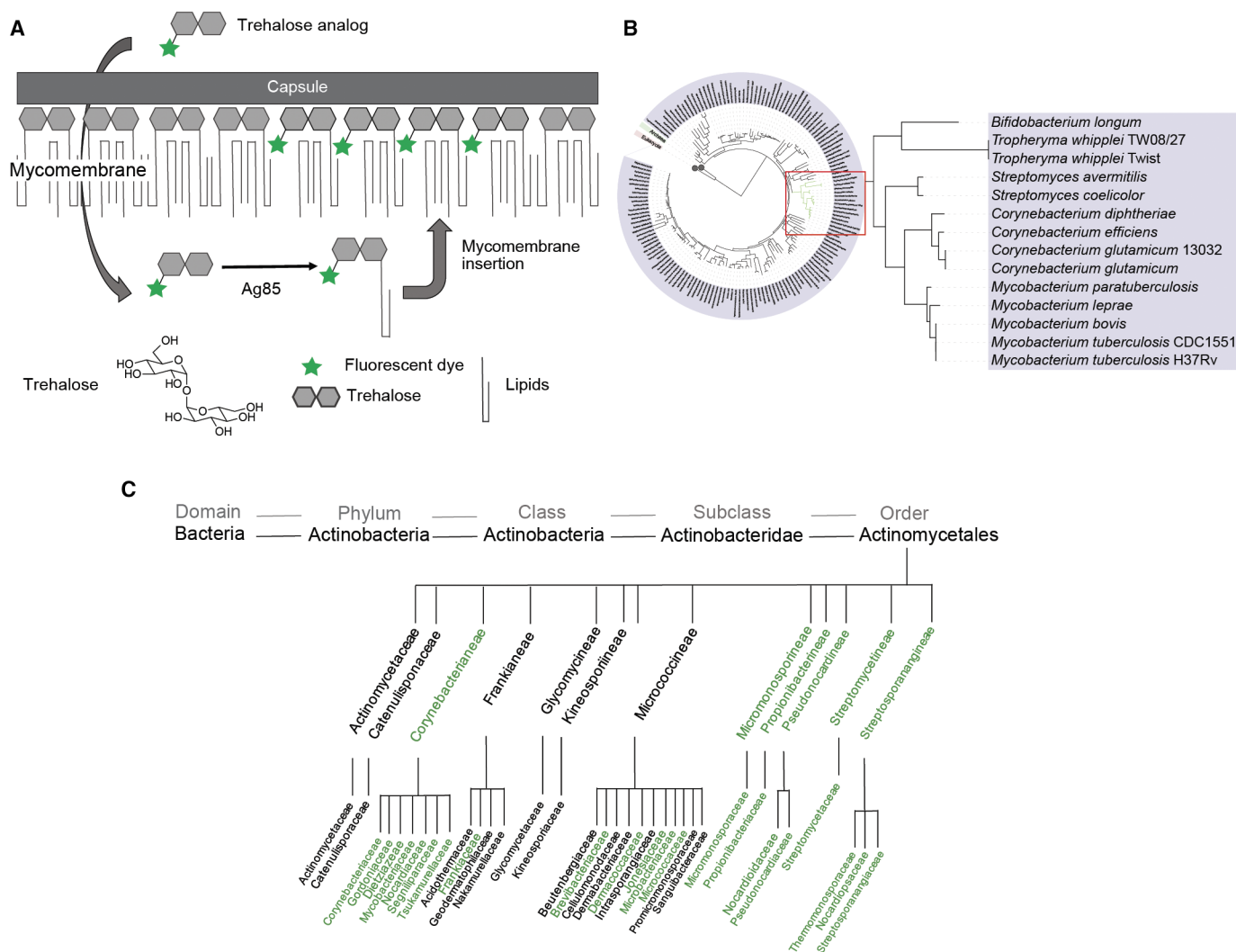


Fig. 1. Strategy for the detection of Actinobacteria by metabolic labeling of the mycomembrane with fluorescent trehalose analogs. (A) Schematic illustration depicting how fluorescent trehalose analogs are converted to trehalose mycolates by the antigen 85 (Ag85) protein complex and incorporated into the mycomembrane of bacteria. (B) Bacterial phylogenetic tree (left) highlighting Actinobacteria that have Ag85 protein homologs (red box). These bacteria (examples listed on right) can potentially incorporate trehalose analogs into the mycomembrane. (C) Representative list of Actinomycetales found (green) or not found (black) in the tblastn search results of unique organisms that may label with trehalose dyes, using the amino acid sequence from the reference proteins fbpA, fbpB, and fbpC. The complete tblastn search results are listed in table S1.

solvents. Accordingly, we reasoned that metabolic mycolylation of DMN-Tre and subsequent integration into the hydrophobic mycomembrane would activate its fluorescence and enable the detection of Mtb cells without the need to wash away unmetabolized probe (Fig. 2A). We synthesized DMN-Tre (1; Fig. 2B) and two control molecules, namely, DMN-glucose (DMN-Glc or 2; Fig. 2B and fig. S1) and 6-fluorescein-trehalose (6-FITre or 3; Fig. 2B) (23). We confirmed that the fluorescence properties of DMN-Tre were similar to those reported for the free dye, including an about 700-fold enhancement in fluorescence intensity when dissolved in 99.9% dioxane versus water (Fig. 2C).

To evaluate the ability of DMN-Tre to label bacteria bearing mycomembranes, we tested several strains from the Actinobacteria phylum. *Mycobacterium smegmatis* (Msmeg), *Corynebacterium glutamicum* (Cg), and *Mycobacterium marinum* (Mm), each in exponential growth phase, were incubated with 100 μ M DMN-Tre (fig. S2) or the non-fluorogenic analog 6-FITre for 1, 2, and 6 hours, respectively, and then imaged without washing. We observed bright fluorescence labeling of all three species with DMN-Tre, with no discernible background fluorescence derived from free DMN-Tre in the surrounding solution (Fig. 3A). In contrast, cells labeled with 6-FITre were obscured by fluorescence of the probe in the surrounding solution. Extensive washing was required to remove nonspecifically bound 6-FITre from cells and their debris, rendering specifically labeled cells difficult to discern compared to those labeled with DMN-Tre. These images were acquired by using standard fluorescein isothiocyanate (FITC)/green fluorescent protein (GFP) filter sets, but an even brighter image could be obtained by excitation at 405 nm, closer to the excitation maximum of DMN (fig. S3).

We performed a time course to determine DMN-Tre labeling kinetics using Msmeg and Cg harvested during their exponential growth phase, incubated with DMN-Tre, and imaged at various time points. As shown in Fig. 3B, labeling was visible at the first time point (5 min for Msmeg and 3 min for Cg). Cg displayed even cell surface labeling by the earliest time point analyzed, whereas Msmeg showed fluorescence only at the polar regions at early time points, consistent with the known polar growth in mycobacterial species (16, 28). This signal eventually spread across the cell length so that, by 1 hour, Msmeg cells were uniformly labeled.

The potential of DMN-Tre as a diagnostic tool for TB depends on its selectivity for mycobacteria, among other bacterial species. We incubated canonical Gram-negative [*Escherichia coli* (Ec)] and Gram-positive [*Staphylococcus aureus* (Sa), *Listeria monocytogenes* (Lm), and *Bacillus subtilis* (Bs)] organisms with DMN-Tre and, without washing, observed no detectable labeling (Fig. 3C and fig. S4). In the same experiment, Cg labeled brightly with DMN-Tre. Further, we combined Msmeg expressing mCherry with the Gram-negative and Gram-positive bacteria in a 1:10 mycobacteria/other bacteria ratio and incubated the mixture with Hoechst dye, a DNA stain, and DMN-Tre for 1 hour. We observed bright, specific, DMN-Tre labeling of only Msmeg cells (Fig. 3D).

DMN-Tre mycolylation is likely mediated by the acyl transferase Ag85 pathway

Next, we performed a series of experiments to confirm that DMN-Tre labeling results from metabolic conversion to trehalose mycolates within the mycomembrane rather than nonspecific insertion into the mycomembrane. By flow cytometry, we confirmed that Msmeg exhibits significant fluorescence over background within 20 min

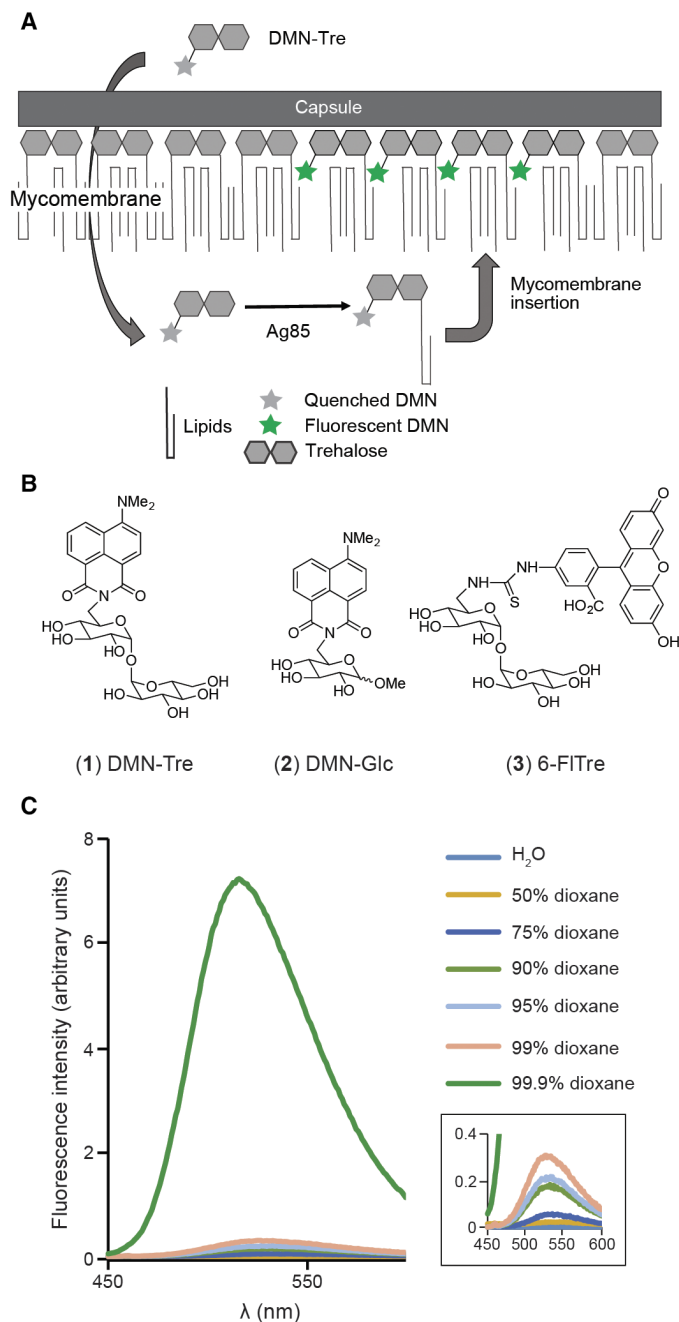


Fig. 2. An environment-sensitive fluorogenic trehalose derivative for the detection of mycobacteria. (A) Schematic illustration depicting the mechanism by which solvatochromic trehalose analogs are converted to trehalose mycolates via the Ag85 complex. Their incorporation into the low dielectric environment of the mycomembrane leads to fluorescence. (B) Structures of 4-*N,N*-dimethylamino-1,8-naphthalimide-conjugated trehalose (DMN-Tre or 1) and control compounds DMN-glucose (DMN-Glc or 2) and 6-fluorescein-trehalose (6-FITre or 3). (C) Fluorescence emission spectra of DMN-Tre in mixtures of dioxane/H₂O. Inset shows enlargement of spectra in $\leq 99\%$ dioxane samples.

(Fig. 4A) and that >70% of cells are labeled within 30 min (Fig. 4B). DMN-Glc, which has the same dye but installed on glucose, did not label Msmeg, suggesting that the trehalose scaffold is key for the

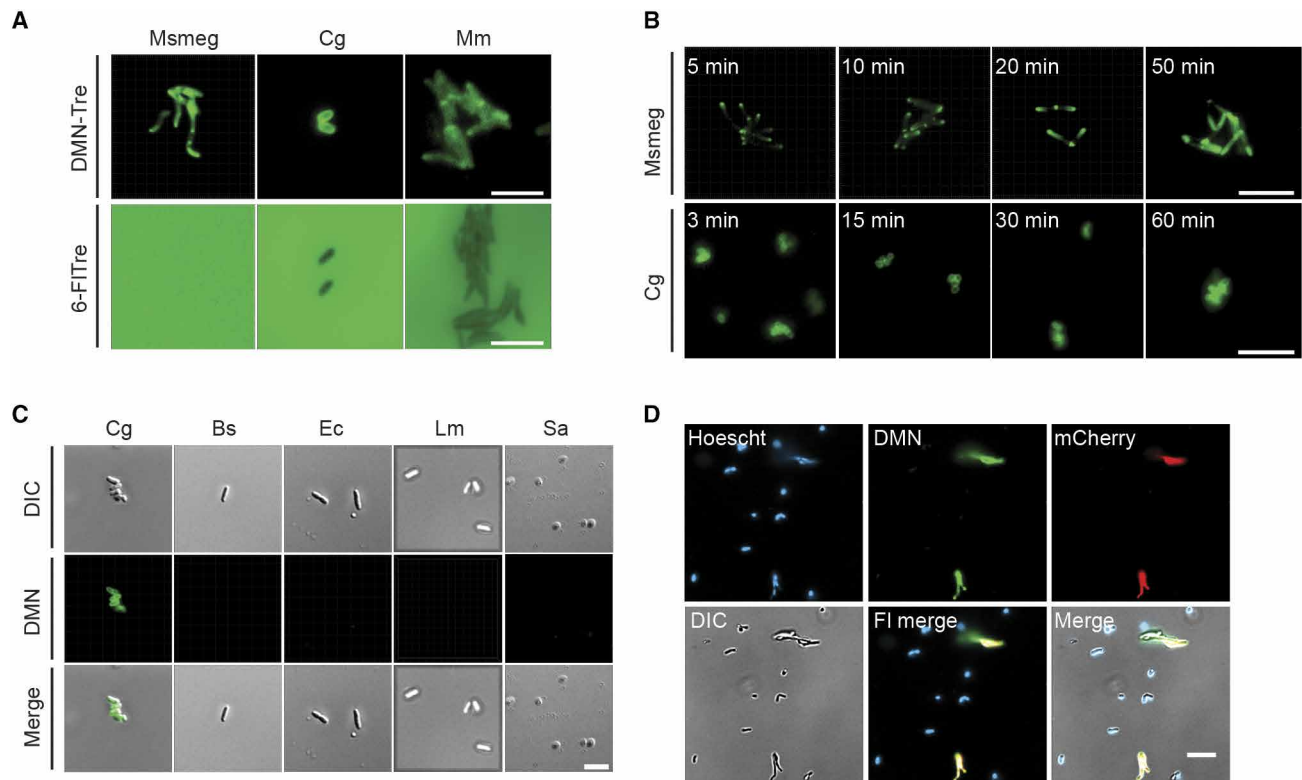


Fig. 3. Specific, no-wash detection of mycobacteria and corynebacteria using DMN-Tre. (A) No-wash imaging of *Mycobacterium smegmatis* (Msmeg), *Corynebacterium glutamicum* (Cg), and *Mycobacterium marinum* (Mm) labeled with 100 μ M DMN-Tre or 6-FITre for 1, 2, and 6 hours, respectively. (B) Fluorescent labeling of Msmeg and Cg by DMN-Tre as a function of time. Cells were directly imaged without washing. (C) No-wash imaging of Cg, *Bacillus subtilis* (Bs), *Escherichia coli* (Ec), *Listeria monocytogenes* (Lm), and *Staphylococcus aureus* (Sa) cells incubated with 100 μ M DMN-Tre for 2 hours. Background fluorescence with non-acid-fast bacteria is minimal under no-wash imaging conditions. (D) Colabeling of mCherry-expressing Msmeg combined with Bs, Ec, Lm, and Sa labeled with 100 μ M DMN-Tre and Hoechst (20 μ g/ml) for 1 hour under no-wash conditions. Images were collected in the differential interference contrast (DIC), 4',6'-diamidino-2-phenylindole (DAPI) (Hoechst fluorescence), fluorescein isothiocyanate (FITC)/green fluorescent protein (GFP) (DMN fluorescence), or red fluorescent protein (RFP) (mCherry fluorescence) channels of a Nikon A1R confocal microscope. "FI merge" represents merged images from the DAPI, GFP, and RFP fluorescence channels. "Merge" represents merged images from all channels. Scale bars, 5 μ m.

fluorescence signal observed with DMN-Tre treatment (Fig. 4C). In addition, DMN-Tre labeling was reduced in the presence of excess trehalose, suggesting competition in the same biosynthetic pathway (Fig. 4D). We also assessed DMN-Tre labeling of a panel of Msmeg trehalose transporter mutants (fig. S5) (29–31) and found that DMN-Tre incorporation does not primarily rely on the intracellular trehalose pathway. This is consistent with metabolism of DMN-Tre occurring within the outer membrane space, the location of Ag85 complex enzymes (16), rather than requiring its import into the cell cytosol.

In addition, we generated an Msmeg mutant that harbors a deletion of the genes MSMEG_6396 to MSMEG_6399, which include genes annotated as Ag85A, Ag85B, and Ag85C (ortholog genes of the Mtb proteins fbpA, fbpB, and fbpD; fig. S6, A and B). In our labeling assay, Δ MSMEG_6396-99 showed a modest but significant (42%) reduction in labeling by DMN-Tre compared to wild type (fig. S6C). Although there may be subtle differences between the activities of Mtb and Msmeg orthologs, these data suggest that DMN-Tre labeling occurs through the Ag85 pathway, consistent with previous studies (17, 20). Accordingly, the Ag85 inhibitor ebselen (32) decreased DMN-Tre labeling of Msmeg cells in a dose-dependent manner (Fig. 4E). Lastly, we analyzed purified glycolipids from DMN-Tre-labeled Cg

by thin-layer chromatography (TLC) (fig. S7A) and mass spectrometry (fig. S7, B to D) and detected DMN-Tre monomycolates as the only identifiably labeled species. The structures of the monomycolates were confirmed by observation of lipid tail fragment loss by tandem mass spectrometry (fig. S8).

Pre-exposure to heat killing or TB drugs inhibits DMN-Tre labeling of Msmeg

Current microscopy-based methods for TB diagnosis cannot distinguish live from dead mycobacteria. Given that DMN-Tre labeling depends on mycomembrane biosynthesis, we hypothesized that this method would be specific for live bacteria. Labeling was abrogated by heat-killing Msmeg (Fig. 5, A and B). In contrast, cultured Msmeg in stationary phase continue to label with DMN-Tre, albeit at lower intensity than Msmeg in log phase (Fig. 5C). An interesting question is whether active Ag85 protein released by live cells (33) can cause mycomembrane labeling of nearby dead cells in the presence of DMN-Tre. We incubated culture filtrates from live Msmeg in growth phase with heat-killed Msmeg cells in the presence of DMN-Tre and analyzed fluorescence of the dead cells by flow cytometry. As shown in Fig. 5D, no such translabeling was observed above the autofluorescence, suggesting that DMN-Tre labeling is cell-autonomous.

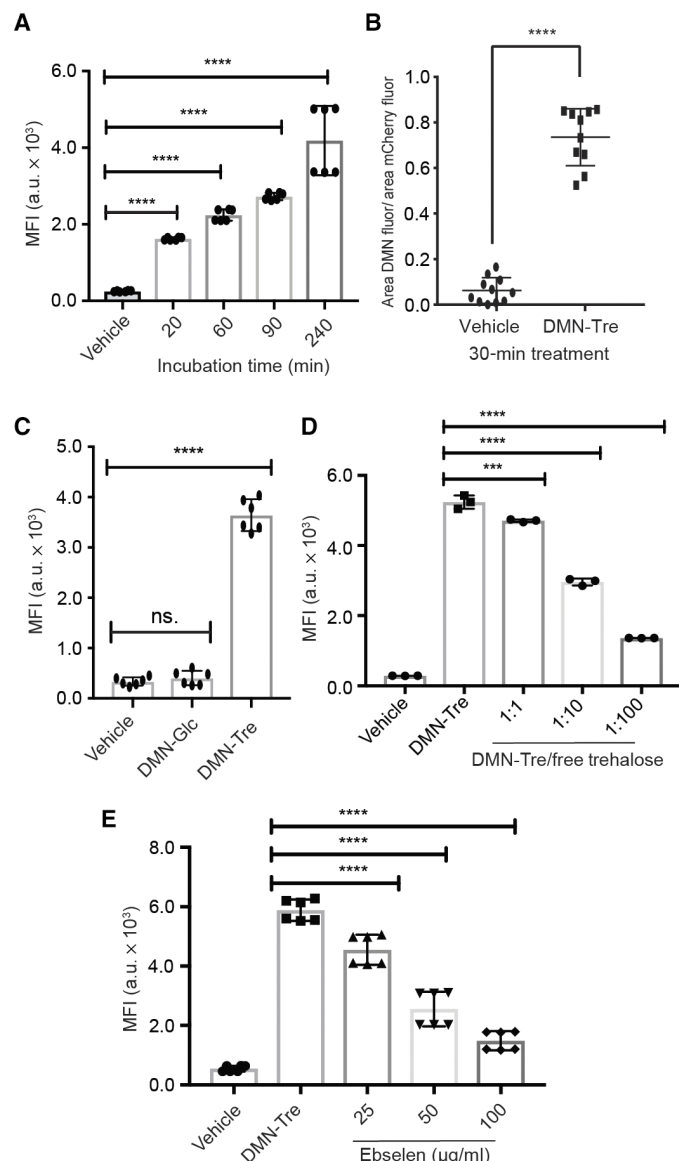


Fig. 4. Labeling of *Msmeg* with DMN-Tre is fast and specific and depends on Ag85A function. (A) Flow cytometry mean fluorescence intensity (MFI) analysis of *Msmeg* labeling time course. Cells were incubated with 100 μ M DMN-Tre for 20, 60, 90, or 240 min. a.u., arbitrary units. (B) Quantitative microscopy analysis of mCherry *Msmeg* cells after incubation with 100 μ M DMN-Tre for 30 min, displaying the ratio of total area of DMN fluorescence over total area of mCherry fluorescence. (C to E) Flow cytometry MFI analysis of *Msmeg* cells (C) incubated for 30 min with 100 μ M DMN-Tre or DMN-Glc and competition of DMN-Tre labeling (D) with free trehalose using the same labeling conditions as in (C); (E) *Msmeg* cells preincubated with ebselen, an Ag85 inhibitor, for 3 hours and labeled with DMN-Tre as in (C). Data are means \pm SEM from at least two independent experiments. Data were analyzed by Student's *t* test in (B) and one-way analysis of variance (ANOVA) test in (A) and (C) to (E) (*****P* < 0.001 and ******P* < 0.0001; ns, not significant).

Next, we evaluated the effect of TB drug treatment on labeling of *Msmeg*. *Msmeg* cells treated for 3 hours with a cocktail of ethambutol, rifampicin, isoniazid, and SQ109, each at a dose at or above reported minimum inhibitory concentrations to induce cell killing (fig. S9), lost detectable labeling with DMN-Tre (Fig. 6, A and B). Because

isoniazid is a prodrug that inhibits mycolic acid biosynthesis after activation by the enzyme KatG (34), we hypothesized that a Δ KatG mutant would be resistant to isoniazid's effects on DMN-Tre labeling. As shown in Fig. 6C, DMN-Tre labeling of Δ KatG mutant of *Msmeg*, but not of wild-type *Msmeg*, was unaffected by isoniazid treatment.

DMN-Tre labeling of *Mtb* is time-dependent and is inhibited by TB drugs

Having established the parameters and mechanistic basis of DMN-Tre labeling with *Msmeg*, we then focused our attention on studies with pathogenic *Mtb*. We incubated *Mtb* H37Rv in liquid culture with 100 μ M DMN-Tre before fixing the cells and visualizing them by fluorescence microscopy (Fig. 7A). The labeling intensity was time-dependent; fluorescent *Mtb* cells became detectable by flow cytometry after 30 min of labeling, and the intensity continued to increase overnight (~16 hours; Fig. 7B) at which point it reached a plateau (fig. S10B). After 30 min of labeling, flow cytometry-based quantitation revealed that >65% of cultured *Mtb* cells were measurably fluorescent (fig. S10A).

We next compared the limit of detection in colony forming units (CFU) per milliliter of DMN-Tre labeling compared to the clinically used auramine staining kit method. We generated serial dilutions of a liquid *Msmeg* cell culture, incubated these samples with 100 μ M DMN-Tre for 1 hour, and then imaged them by fluorescence microscopy. We consistently detected fluorescent cells at cell densities as low as 10,000 CFU/ml. This value is on par with published reports of the limit of detection of the auramine staining method (also ~10,000 CFU/ml) (35).

We then assessed the effects of TB drug treatment on DMN-Tre labeling of *Mtb* and the possible labeling of drug-compromised cells by exogenous Ag85 released from neighboring cells. Similar to our observations with *Msmeg*, treatment of *Mtb* cells with the drug cocktail for 3 hours before incubation with DMN-Tre led to a reduction in cell viability (fig. S11A) and reduced DMN-Tre labeling (Fig. 7C and fig. S11B). In contrast, labeling with auramine was unaffected by prior drug cocktail treatment (Fig. 7D). In addition, we incubated culture filtrates from live H37Rv *Mtb* in growth phase with rifampin-compromised *Mtb* samples in the presence of DMN-Tre and analyzed fluorescence of the drug-treated cells by flow cytometry. As shown in fig. S12, the addition of culture filtrates from live cells did not enhance labeling of rifampin-treated cells, confirming that DMN-Tre labeling of mycobacteria is cell-autonomous.

DMN-Tre detects *Mtb* in sputum samples from patients with TB

Finally, to gain insight into the potential clinical utility of DMN-Tre, we sought to detect *Mtb* cells in sputum samples from treatment-naïve patients who were TB-positive either by smear microscopy or by GeneXpert analysis. The samples were decontaminated using a standard *N*-acetyl-L-cysteine/sodium hydroxide (NALC/NaOH) treatment and then incubated with DMN-Tre (Fig. 8A). Initially, sputum samples were imaged after a 2-hour incubation with DMN-Tre, and fluorescent *Mtb* cells were readily visible in all samples (Fig. 8B). Subsequently, we performed a small-scale smear test comparison between DMN-Tre and Auramine O stain. For the 16 sputum samples collected, each was split in half, and the samples were incubated with DMN-Tre for 30 min or smeared with Auramine O stain according to standard kit protocol. We detected *Mtb* cells in these samples with

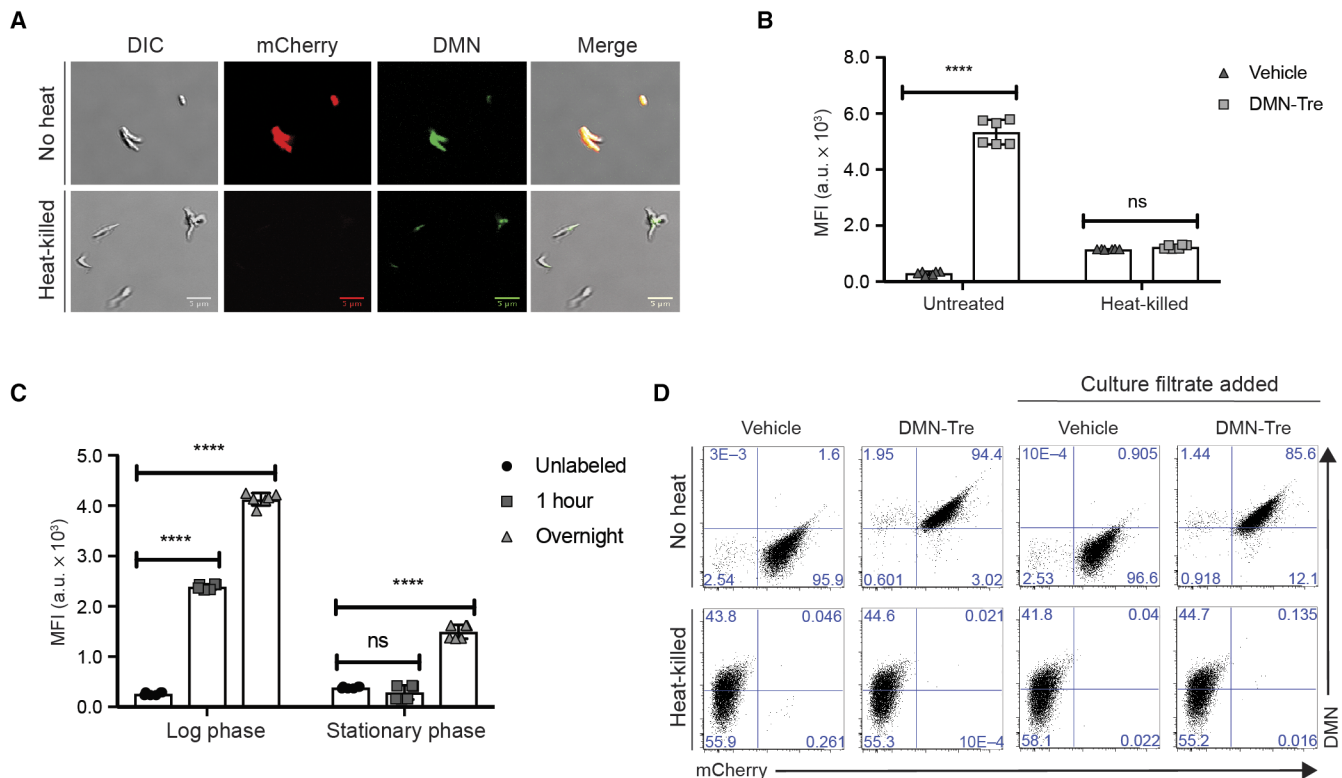


Fig. 5. DMN-Tre labeling is selective for live mycobacteria. (A and B) No-wash imaging (A) and flow cytometry MFI analysis (B) of live and heat-killed (95°C for 30 min) mCherry Msmeg cells in the presence of 100 μ M DMN-Tre for 30 min. (C) Flow cytometry MFI analysis of Msmeg cells in exponential (log) or stationary growth phase incubated with 100 μ M DMN-Tre for 1 hour or overnight (~16 hours). (D) Flow cytometry analysis of live or heat-killed cells resuspended with or without culture filtrates from live cells, followed by incubation with DMN-Tre as in (A). Images were collected in the DIC, FITC/GFP (for DMN fluorescence), or RFP (for mCherry fluorescence) channels of a Nikon A1R confocal microscope. Scale bars, 5 μ m. In (B) and (C), data are means \pm SEM from at least two independent experiments. Data were analyzed by two-way ANOVA test (**** P < 0.0001).

both reagents, although the no-wash DMN-Tre procedure was considerably simpler than the multistep auramine procedure (Fig. 8C). For each reagent, we quantified the number of visibly stained cells over eight fields of view per sample for all 16 sputum samples (Fig. 8D and fig. S13). DMN-Tre performed similarly to Auramine O in terms of the number of Mtb cells detected in sputum from these patients before drug treatment.

DISCUSSION

The World Health Organization has articulated the urgent need for new sputum tests for rapid TB diagnosis (2). Several groups have taken on this challenge with a variety of approaches. For example, Rao and co-workers (36, 37) developed an enzyme-activated fluorogenic probe that reports spectroscopically on Mtb-specific β -lactamase activity. The test can detect Mtb in sputum samples, although its sensitivity to cell viability or drug susceptibility was not reported.

Given that microscopy-based tests still far outnumber other diagnostic platforms in low-resource settings, methods for imaging Mtb cells in sputum are of particular interest (38). Datta and co-workers (39) reported that the vital dye fluorescein diacetate can be used in conjunction with auramine staining to monitor the response of TB to front-line therapy in patients. However, the fluorescent probe does not have good specificity for Mtb since others have reported its

use for staining both Gram-positive and Gram-negative bacteria (40–42).

DMN-Tre labeling appears to be unique in its combination of attributes. Unlike classic methods for detecting Mtb cells by microscopy, DMN-Tre labeling specifically targets a pathway in mycomembrane biosynthesis and, therefore, reports both on bacterial identity and on metabolic viability. This specificity is striking, given the important role that free trehalose plays as an osmo- and thermoprotectant in other bacterial species (43, 44). The unique solvatochromic property of DMN-Tre enables rapid Mtb imaging without washing steps. These features enable the rapid detection of Mtb in complex samples, such as patient sputum.

DMN-Tre labeling may also report on drug sensitivity. The current practices for determining drug susceptibility of clinical Mtb isolates either are polymerase chain reaction–based for known resistance genes or require lengthy (up to 6 weeks) culturing of samples in the presence of drugs (45). Our preliminary studies with a TB drug cocktail indicate that DMN-Tre labeling is affected by drug action within hours, and the results of such a microscopy test could therefore be available on the same day as sample collection. Although our results suggest that DMN-Tre can distinguish metabolically active versus inactive organisms, further studies are warranted to assess whether DMN-Tre distinguishes live versus dead cells. It will be particularly interesting to determine whether nonreplicating or “dormant” Mtb cells are detectable

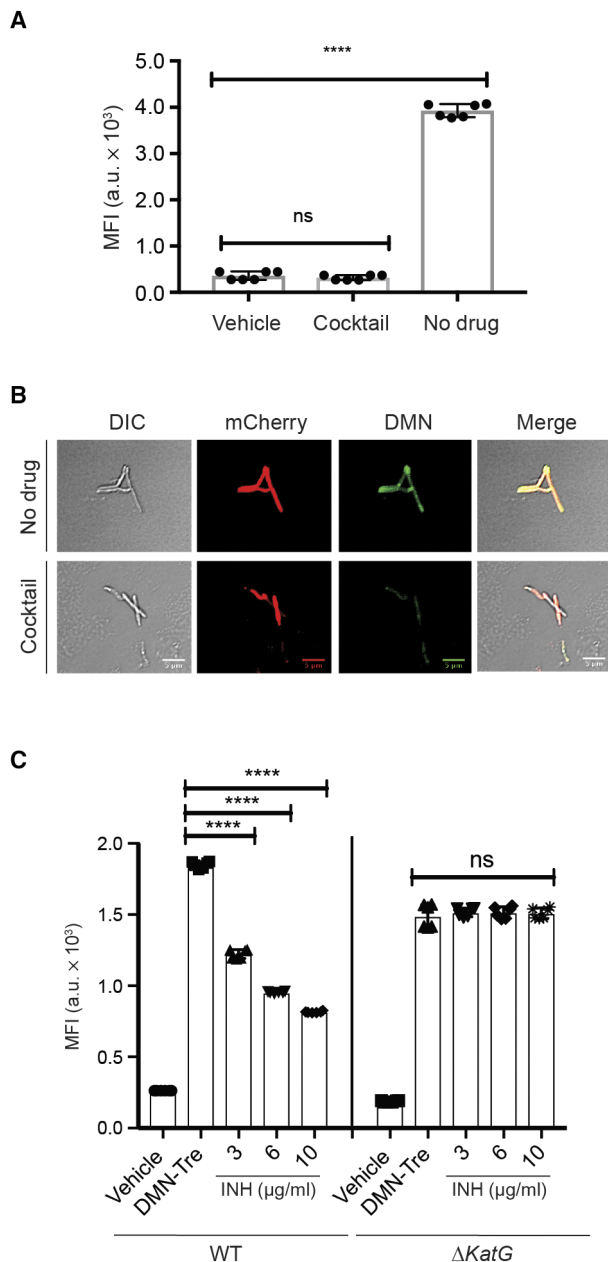


Fig. 6. DMN-Tre labeling is inhibited by tuberculosis drugs. (A and B) Flow cytometry MFI analysis (A) and no-wash imaging (B) of control and drug-treated (37°C for 3 hours) *Msmeg* cells labeled with 100 µM DMN-Tre for 30 min. Drug cocktail contents: ethambutol (1 µg/ml), rifampicin (0.2 µg/ml), SQ109 (20 µg/ml), and isoniazid (20 µg/ml) in 7H9 medium. (C) Flow cytometry MFI analysis of wild-type (WT) *Msmeg* or *KatG* mutant cells treated with isoniazid (INH) at the indicated final concentrations (0, 3, 6, or 10 µg/ml of isoniazid) for 3 hours, followed by incubation with DMN-Tre for 30 min. Images were collected in the DIC, FITC/GFP (for DMN fluorescence), or RFP (for mCherry fluorescence) channels of a Nikon A1R confocal microscope. Scale bars, 5 µm. In (A) and (C), data are means ± SEM from at least two independent experiments. Data were analyzed by one-way ANOVA test (*****P* < 0.0001).

with this method. In addition, a larger clinical study is needed to validate the utility of DMN-Tre to monitor drug efficacy during TB treatment.

The unique mode of fluorescence activation of DMN-Tre allows for an operationally simple procedure—a single incubation step. Notably,

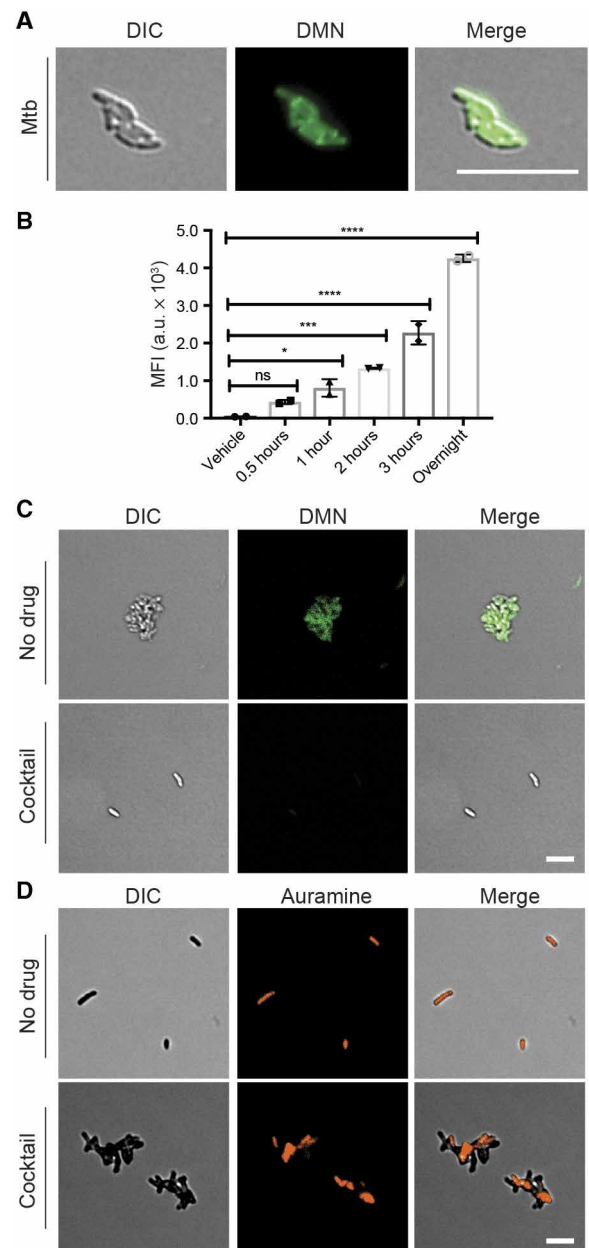


Fig. 7. DMN-Tre labeling of *Mycobacterium tuberculosis* is inhibited by tuberculosis drug cocktail, unlike auramine staining. (A) Microscopy analysis of *Mycobacterium tuberculosis* (Mtb) cells incubated with 100 µM DMN-Tre for 2 hours. (B) Flow cytometry MFI analysis of Mtb cells incubated with DMN-Tre for the indicated times: 0.5, 1, 2, and 3 hours or overnight (~16 hours). Error bars denote three biological replicates. (C and D) Microscopy analysis of control and drug-treated Mtb cells labeled with 100 µM DMN-Tre overnight (C) or stained with the auramine-based Fluorescent Stain kit for mycobacteria (05151, Sigma-Aldrich) (D). Drug cocktail contents: ethambutol (1 µg/ml), rifampicin (0.2 µg/ml), SQ109 (10 µg/ml), and isoniazid (10 µg/ml) in 7H9 medium. Images were collected in the DIC or FITC/GFP (for DMN and Auramine fluorescence) channels of a Nikon A1R confocal microscope. Cells stained with auramine were given an orange pseudocolor. Scale bars, 5 µm. In (B), data are means ± SEM from at least two independent experiments. Data were analyzed by one-way ANOVA test (**P* < 0.05, *****P* < 0.001, and *****P* < 0.0001).

we found DMN-Tre to be very stable on the bench or in shipping containers for weeks at room temperature and even in aqueous solution at 37°C. Thus, the DMN-Tre labeling procedure may translate

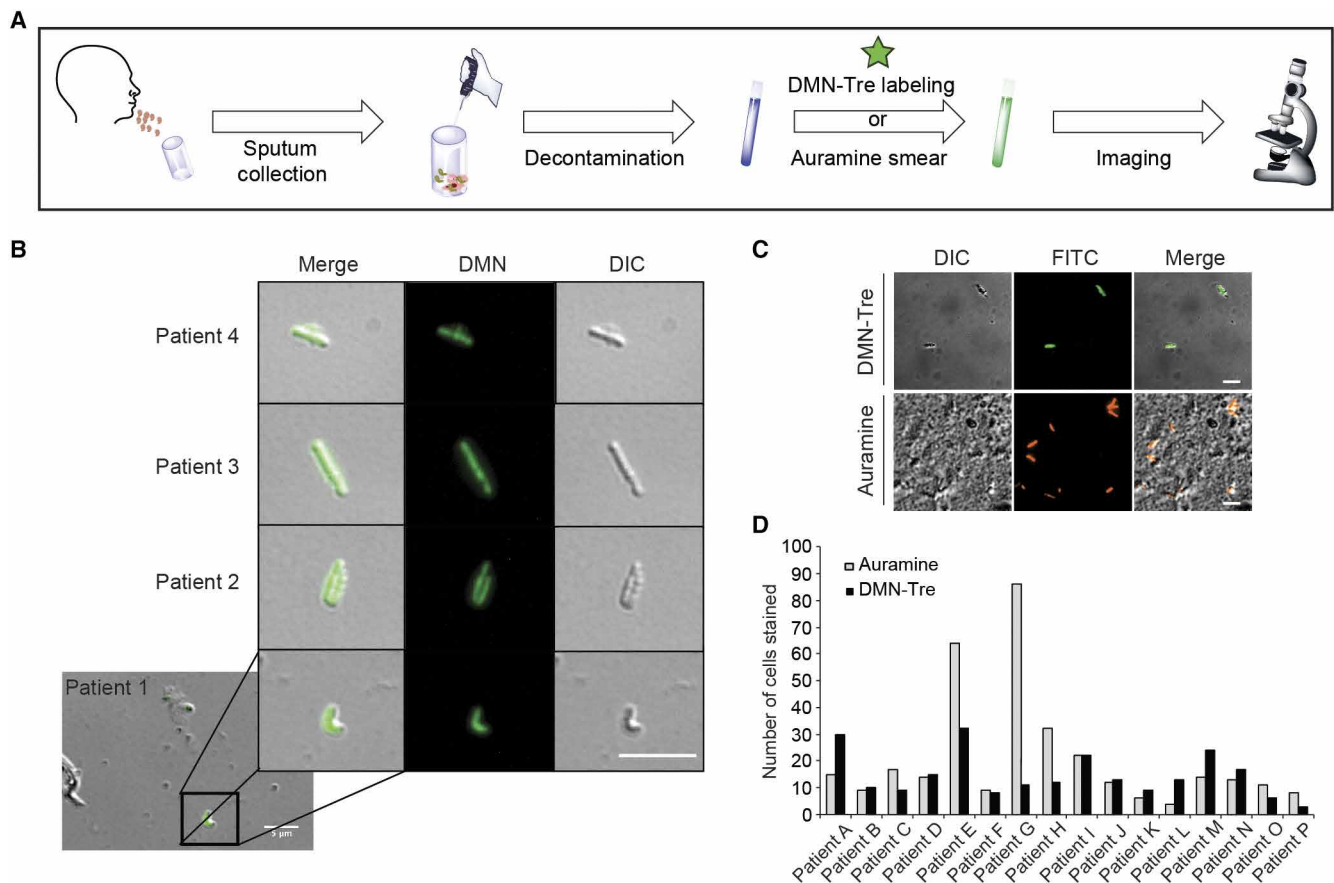


Fig. 8. DMN-Tre detects Mtb in sputum samples from patients with tuberculosis, similar to the auramine stain. (A) Illustration of sputum sample labeling protocol: 16 sputum samples were collected from diagnosed treatment-naïve patients with tuberculosis and were decontaminated with *N*-acetyl-L-cysteine (NALC)/NaOH mixture following recommended standards. Decontaminated sputum samples were split in two equal aliquots, each incubated with 1 mM DMN-Tre or smeared with Auramine O stain, followed by imaging. (B) Microscopy analysis of four decontaminated sputum samples incubated with 1 mM DMN-Tre in 7H9 liquid medium for 2 hours in a 37°C atmospheric incubator. (C) Microscopy analysis of decontaminated sputum samples either treated with 1 mM DMN-Tre for 30 min at 37°C (top) or directly fixed onto microscope slide for Auramine O staining following standard kit protocol (bottom, orange pseudocolor). (D) Bar graph depiction of the total Mtb cell number detected over eight fields of view per sample with either DMN-Tre or Auramine O in the 16 sputum samples treated as in (C). Images were collected in the DIC and FITC (for DMN and auramine fluorescence) channels of a Zeiss Observer Z1-inverted fluorescent microscope. Scale bars, 5 µm.

well both to research and to clinical applications in low-resource environments.

MATERIALS AND METHODS

Study design

The objective of the study was to assess the utility of a solvatochromic trehalose conjugate dye for the detection of mycobacteria and corynebacteria, along with its potential applications in medicine. The fluorogenic DMN-Tre conjugate was synthesized, and its fluorescence and labeling capabilities were assessed in comparison to already published fluorescent trehalose dyes. Given the potential of DMN-Tre as a rapid stain, DMN-Tre was tested against various mycobacterial, corynebacterial, and bacterial strains to assess its specificity. Furthermore, DMN-Tre was tested against a diversity of control groups and subjected to tandem mass spectrometry to validate probe incorporation into the mycobacterial cell wall. Next, we assayed the pathway required for DMN-Tre labeling by testing several mutant strains known to be involved in cell wall biosynthesis. Then, we validated the ne-

cessity for active metabolism by subjecting the mycobacteria to heat killing or TB drug treatment before DMN-Tre labeling and detection. DMN-Tre labeling of Mtb was assessed by fluorescence microscopy and flow cytometry and then compared to detection of Mtb with auramine staining in the context of TB drug treatment. Finally, a small sample of 16 patients diagnosed with TB provided sputum samples that were subjected to DMN-Tre labeling and assessed for detection of labeled Mtb cells by microscopy. Ethics approval for the study was provided by the University of the Witwatersrand Human Research Ethics Committee (clearance no. M110833).

Metabolic labeling of bacteria with DMN-Tre, DMN-Glc, or 6-FITre

Cultures of *Msmeg* or mutants were made by inoculation of a single colony from an agar plate into BD Difco Middlebrook 7H9 (catalog no. DF0713-17-9, Thermo Fisher Scientific) liquid broth (1 ml) supplemented with 10% (v/v) oleate-albumin-dextrose-catalase (OADC) enrichment (BBL Middlebrook OADC, catalog no. 212351), 0.5% (v/v) glycerol, and 0.05% (w/v) Tween 80 (P1754, Sigma-Aldrich)

with or without antibiotic (if necessary) in a 5-ml culture tube (14-959-11B, Thermo Fisher Scientific). Cultures of Cg, Bs, Ec, Lm, and Sa were generated by inoculation of a single colony from an agar plate into LB (1 ml; 12795-084, Invitrogen) liquid medium in a 5-ml culture tube. Cultures of Mtb were made by inoculation of a 1-ml frozen stock into 50 ml of Middlebrook 7H9 liquid medium supplemented with 10% (v/v) OADC enrichment (BBL Middlebrook OADC, 212351), 0.5% (v/v) glycerol, and 0.05% (w/v) Tween 80 (P1754, Sigma-Aldrich) in a roller bottle or a tissue culture flask. Cultures were grown to an optical density at 600 nm (OD_{600}) of 0.5 to begin the experiments. Bacterial cultures were mixed with DMN-Tre, DMN-Glc, or 6-FITre at a final concentration of 100 μ M in 7H9 medium and incubated at 37°C with shaking or rolling for an additional one doubling time (unless otherwise specified). Vehicle controls were obtained from cells treated in an identical fashion in the absence of fluorescent probes. For Mtb, labeled cells were harvested by centrifugation (3000g for 10 min) and then fixed in an equal volume of 2.5% glutaraldehyde (room temperature for 1 hour, with occasional rotation of the tube to ensure sterilization of all internal surfaces before fluorescence analysis).

Flow cytometry

After metabolic labeling and fixation (for Mtb cells), cells were harvested by centrifugation (3300g for 3 min), washed [two washes of 500 μ l with 1 \times Dulbecco's phosphate-buffered saline (DPBS; MT-21-030-CV, Thermo Fisher Scientific)], and resuspended in 300 μ l of 1 \times DPBS. Fluorescence measurements were taken in 5-ml culture tubes (14-959A, Thermo Fisher Scientific) suitable for flow cytometry. Data collection was performed on a BD LSR II UV instrument in the shared Fluorescence Activated Cell Sorting (FACS) Facility at Stanford University. This instrument is equipped with a 405-nm violet laser and 488-nm blue laser for Aqua Amine and FITC channels, respectively, both used to detect DMN-Tre fluorescence. Fluorescence data were obtained for 100,000 cells per sample and processed using FlowJo (Tree Star) software. Experiments were conducted in three biological replicates.

Fluorescence microscopy

After metabolic labeling and fixation (for Mtb cells), 6 μ l of cell suspension was spotted onto slides, covered with coverslips, and sealed with adhesive. Microscopy was performed on a Nikon A1R confocal microscope equipped with a Plan Fluor 60 \times oil immersion 1.30-numerical aperture objective. This instrument is equipped with a 405-nm violet laser, 488-nm blue laser, and 561-nm green laser for Aqua Amine, FITC/GFP, and red fluorescent protein (RFP) channels, respectively. NIS-Elements AR software (Nikon Inc.) was used to process images. All image acquisition and processing were executed under identical conditions for control and test samples.

Absorbance and fluorescence measurements of DMN-Tre

One microliter of 10 mM DMN-Tre in H₂O was added to 1 ml of mixtures of dioxane and water at different ratios. Absorbance spectra were recorded on a Varian Cary 50 UV-Visible spectrophotometer. Fluorescence spectra were recorded on a Photon Technology International Quanta Master 4 L-format scanning spectrofluorometer equipped with an LPS-220B 75-W xenon lamp and power supply, an A-1010B lamp housing with an integrated igniter, a switchable 814 photon-counting/analog photomultiplier detection unit, and an MD5020 motor driver. Measurements were made in 1 cm \times 0.4 cm quartz cuvettes with a total sample volume of 1 ml.

No-wash imaging of Msmeg, Cg, and Mm by DMN-Tre and 6-FITre

Msmeg or Cg was grown to an OD_{600} of 0.5 from a single colony (37°C for Msmeg and 30°C for Cg). Five microliters of 10 mM DMN-Tre or 10 mM 6-FITre in H₂O was added to 500 μ l of culture. The bacteria were incubated for another 1 hour (Msmeg) or 2 hours (Cg), then placed on a microscope slide (under a coverslip), and imaged directly. Mm was stored as an OD_{600} = 0.5 stock in 50% glycerol/50% 7H9 + OADC. One milliliter of this frozen culture was thawed, and the bacteria were pelleted (3300g for 3 min) and resuspended in 2 ml of 7H9 liquid medium supplemented with 10% (v/v) OADC enrichment (BBL Middlebrook OADC, 212351), 0.5% (v/v) glycerol, and 0.05% (w/v) Tween 80 (P1754, Sigma-Aldrich). The bacteria were incubated at 33°C overnight (~16 hours). Five microliters of 10 mM DMN-Tre or 10 mM 6-FITre in H₂O was added to 500 μ l of Mm culture. The bacteria were incubated at 33°C for 6 hours, then placed under a coverslip, and imaged without washing.

No-wash labeling of Msmeg and Cg over time

Msmeg or Cg cells were grown to an OD_{600} of 0.5 from a single colony, as described in "No-wash imaging of Msmeg, Cg and Mm by DMN-Tre and 6-FITre" section above. Two microliters of 10 mM DMN-Tre in H₂O was added to 200 μ l of culture. Aliquots were taken from this culture at the indicated time points, immediately placed under a coverslip, and imaged.

Labeling of non-mycomembrane-bearing bacteria

Lm, Bs, Ec, and Sa were grown from single colonies at 37°C overnight. The bacteria were diluted to an OD_{600} of 0.4. Ten microliters of 10 mM DMN-Tre was added to 1 ml of aliquots of these bacteria to reach a final concentration of 100 μ M DMN-Tre. The cells were then incubated at 37°C for 2 hours. Aliquots were taken, and the cells were imaged under a coverslip. As controls, cells from the same OD_{600} = 0.4 culture, without the addition of DMN-Tre, were also imaged.

Selective labeling of Msmeg in the presence of other bacterial species

Bacteria (Lm, Bs, Ec, and Sa) were grown overnight in medium, with shaking, as noted above. The bacteria were diluted to an OD_{600} of 0.5, and then, 500 μ l of each culture was mixed together to create 2 ml of mixed bacteria. One milliliter of Msmeg expressing mCherry was grown from a single colony overnight to an OD_{600} of 0.5. Both cultures were pelleted by centrifugation (3300g for 3 min) and resuspended in an identical volume of LB medium. Sixty microliters of Msmeg was added to 540 μ l of mix. Lastly, this final mixture of bacteria containing Msmeg and the four other non-mycomembrane-bearing bacterial species was split into two 300 μ l of aliquots. To each group, 0.3 μ l of Hoechst DNA stain (2 mg/ml; 62249, Thermo Fisher Scientific) was added to stain all the bacteria. To one of the two aliquots, 3 μ l of 10 mM DMN-Tre was added, whereas no DMN-Tre was added to the other portion. The two aliquots were incubated with shaking at 37°C for 1 hour before a sample was taken out and imaged without washing.

Trehalose competition of DMN-Tre labeling in Msmeg

Msmeg was grown to an OD_{600} of 0.4 from a single colony, as noted above. Then, the bacteria were divided into 100 μ l of aliquots. One microliter of 10 mM DMN-Tre and 1 μ l of 0, 10 or 100 mM trehalose in water were added to these aliquots. The bacteria were grown

for another 1 hour, washed twice with PBS, resuspended in PBS, and examined by flow cytometry and microscopy.

Ebselen inhibition studies

Msmeg was grown to an OD₆₀₀ of 0.4 from a single colony, as noted above. Then, 500 µl of aliquots of bacterial culture was incubated with ebselen (25, 50, or 100 µg/ml; 60940-34-3, Sigma-Aldrich) for 3 hours. Five microliters of 10 mM DMN-Tre was added to these pretreated samples. The cultures were grown for another 1 hour, washed twice with DPBS, resuspended in DPBS, and examined by flow cytometry and microscopy.

Growth phase studies

Msmeg was grown from a single colony to an OD₆₀₀ of 0.5 or greater than 2. Then, 500 µl of aliquots of bacterial culture was incubated with 5 µl of 10 mM DMN-Tre for 30 min, washed twice with PBS, resuspended in DPBS, and examined by flow cytometry and microscopy.

DMN-Tre labeling of drug-treated Msmeg and Mtb

Msmeg was grown to an OD₆₀₀ of 0.4 from a single colony, as noted above. Then, 500 µl of aliquots of bacterial culture was incubated with control or drug cocktail [ethambutol (1 µg/ml; E4630, Sigma-Aldrich), rifampicin (0.2 µg/ml; 1604009, Sigma-Aldrich), SQ109 (10 µg/ml; A3834, ApexBio), and isoniazid (10 µg/ml; I3377, Sigma-Aldrich) in 7H9 medium] for 3 hours in a 37°C atmospheric incubator. Five microliters of 10 mM DMN-Tre was added to these pretreated samples. The cultures were grown for another 30 min, washed twice with DPBS, resuspended in DPBS, and examined by flow cytometry and microscopy.

For Mtb, cultures were made by inoculation of a 1-ml frozen stock into 50 ml of Middlebrook 7H9 liquid medium supplemented with 10% (v/v) OADC enrichment (BBL Middlebrook OADC, 212351), 0.5% (v/v) glycerol, and 0.05% (w/v) Tween 80 (P1754, Sigma-Aldrich) in a roller bottle. Cells were grown to an OD₆₀₀ of 0.5 to begin the experiments. Five hundred microliters of aliquots of bacterial culture was incubated with control or drug cocktail [ethambutol (1 µg/ml), rifampicin (0.2 µg/ml), SQ109 (10 µg/ml), and isoniazid (10 µg/ml) in 7H9 medium] for 3 hours in a 37°C atmospheric incubator, followed by incubation with 100 µM DMN-Tre overnight (~16 hours). Labeled cells were harvested by centrifugation (3000g for 10 min) and then fixed in an equal volume of 2.5% glutaraldehyde (the cells were incubated at room temperature for 1 hour, with occasional rotation of the tube to ensure sterilization of all internal surfaces before fluorescence and flow cytometry analysis).

Patient recruitment and sputum sample collection

Ethics approval for the study was provided by the University of the Witwatersrand Human Research Ethics Committee (clearance no. M110833). Participants for the study were approached at primary health care clinics; those who were willing to participate ($n = 16$) were then asked to visit the study clinic where informed consent was administered.

The enrollment criteria were as follows: (i) 18 years or older, (ii) able to produce a sputum sample of at least 3 to 5 ml, (iii) a hard copy of an HIV test result (HIV-seronegative results dating from within 2 months of enrollment accepted), and (iv) no previous treatment for TB.

The exclusion criteria were as follows: (i) rifampicin mono- or multi-drug resistance, (ii) unable to produce an overnight baseline sputum of 3 to 5 ml or greater, and (iii) any clinical or social characteristic suggesting that the patient will not complete their TB treatment.

Thereafter, a spot or overnight sputum sample was collected and transported to the laboratory for processing. Sputum was decontaminated by the addition of an equal volume of 2.9% sodium citrate and 4% sodium hydroxide (NaCl/NaOH), followed by incubation at room temperature for 20 min. Thereafter, the bacterial cells were harvested at 3900g for 10 min and washed with 4.5 ml of 0.01 M 1× PBS (pH 7.4), followed by resuspension in 2 ml of Middlebrook 7H9 medium supplemented with 0.5% Tween and OADC (Becton Dickinson). To disperse clumps, cells were vortexed briefly in the presence of 2-mm glass beads.

Microscopy analysis of Mtb in sputum samples

Ten microliters of 10 mM DMN-Tre was added to 0.1 ml of aliquots of isolated, decontaminated sputum samples from patients with TB to reach a final concentration of 1 mM DMN-Tre. Samples were then incubated at 37°C for the indicated times (Fig. 8). Samples were fixed in a final concentration of 2.5% glutaraldehyde and incubated at room temperature for 1 hour, with occasional rotation of the tube to ensure sterilization of all internal surfaces. Before imaging, samples were resuspended in 30 µl of 1× PBS.

Auramine versus DMN-Tre smear test

Auramine smear was performed according to standard protocol included in the kit (Fluorescent Stain Kit for mycobacteria, 05151, Sigma-Aldrich). Briefly, one-half of NaCl/NaOH-decontaminated sputum sample was smeared onto microscopy slides and heat-fixed (heating block, 95°C; 5 to 10 min). Smears were then treated with Auramine O for 5 min, destained, and then counterstained before viewing in the FITC/GFP channel using a Zeiss Observer Z1-inverted fluorescence microscope.

For DMN-Tre labeling, the other half of the same sample was stained as follows: 100 µl of sample was incubated with 1 mM DMN-Tre for 30 min at 37°C, followed by fixing in 2.5% glutaraldehyde for 1.5 hours. Samples were then resuspended in 30 µl of 1× PBS. Twenty microliters was mounted on a 2% agarose pad for viewing in the FITC and differential interference contrast channels of a Zeiss Observer Z1-inverted fluorescence microscope.

Statistical analysis

Data are means ± SEM from at least two independent experiments. Unless otherwise specified, all data were analyzed using GraphPad Prism software's ANOVA (analysis of variance) test, as specified in the figure legends.

SUPPLEMENTARY MATERIALS

www.sciencetranslationalmedicine.org/cgi/content/full/10/430/eaam6310/DC1

Materials and Methods

Fig. S1. Synthesis of DMN-Tre and DMN-Glc.

Fig. S2. DMN-Tre labeling is concentration-dependent.

Fig. S3. Optimization of DMN-Tre detection.

Fig. S4. DMN-Tre labeling is specific to bacteria bearing mycomembranes.

Fig. S5. DMN-Tre labeling does not primarily rely on the intracellular trehalose metabolic pathway.

Fig. S6. Msmeg ΔMSMEG_6396-6399 gene deletion mutant exhibits reduced labeling with DMN-Tre.

Fig. S7. DMN-Tre is incorporated into trehalose monomycolate in the mycobacterial outer membrane.

Fig. S8. Loss of lipid tails from DMN-Tre-corynemonomycolates is detected by tandem mass spectrometry.

Fig. S9. Drug cocktail kills Msmeg cells in vitro.

Fig. S10. DMN-Tre time course labeling of H37Rv axenic cultures.

Fig. S11. Drug cocktail kills Mtb cells and inhibits DMN-Tre incorporation into the mycomembrane.

Fig. S12. Rifampin-treated Mtb cells do not label with DMN-Tre, even in the presence of culture filtrates from live Mtb cells.

Fig. S13. DMN-Tre detects Mtb cells in sputum samples comparably to auramine staining.

Table S1. List of strains with Ag85 homology.

Appendix S1. ¹H and ¹³C nuclear magnetic resonance spectra.

Reference (46)

REFERENCES AND NOTES

- World Health Organization (WHO), "Global tuberculosis report 2016" (WHO Press, 2016); <http://apps.who.int/iris/bitstream/10665/250441/1/9789241565394-eng.pdf>.
- World Health Organization (WHO), "High-priority target product profiles for new tuberculosis diagnostics: Report of a consensus meeting" (WHO Press, 2014); http://apps.who.int/iris/bitstream/10665/135617/1/WHO_HTM_TB_2014.18_eng.pdf.
- World Health Organization (WHO), "Molecular line probe assays for rapid screening of patients at risk of multidrug-resistant tuberculosis (MDR-TB)" (WHO Press, 2008) www.who.int/tb/features_archive/policy_statement.pdf.
- L. M. Parsons, Á. Somoskövi, C. Gutierrez, E. Lee, C. N. Paramasivan, A. Abimiku, S. Spector, G. Roscigno, J. Nkengasong, Laboratory diagnosis of tuberculosis in resource-poor countries: Challenges and opportunities. *Clin. Microbiol. Rev.* **24**, 314–350 (2011).
- F. Ziehl, Zur färbung des tuberkelbacillus. *Dtsch. Med. Wschr.* **8**, 451 (1882).
- F. Ziehl, Ueber die färbung des tuberkelbacillus. *Dtsch. Med. Wschr.* **9**, 247–249 (1883).
- F. Neelsen, Ein casuistischer beitrag zur lehre von der tuberkulose. *Centralbl. Med. Wissensch.* **28**, 497–501 (1883).
- P. K. H. Hagemann, Fluoreszenzfärbung von tuberkelbakterien mit auramin. *Münch. Med. Wschr.* **85**, 1066–1068 (1938).
- J. C. Boyd, J. J. Marr, Decreasing reliability of acid-fast smear techniques for detection of tuberculosis. *Ann. Intern. Med.* **82**, 489–492 (1975).
- J. P. Truant, W. A. Brett, W. Thomas Jr., Fluorescence microscopy of tubercle bacilli stained with auramine and rhodamine. *Henry Ford Hosp. Med. Bull.* **10**, 287–296 (1962).
- C. F. F. C. Filho, M. G. F. Costa, Sputum smear microscopy for tuberculosis: Evaluation of autofocus functions and automatic identification of tuberculosis mycobacterium, in *Understanding Tuberculosis—Global Experiences and Innovative Approaches to the Diagnosis*, P. J. Cardona, Ed. (InTech, 2012), chap. 13.
- R. Singhal, V. P. Myneedu, Microscopy as a diagnostic tool in pulmonary tuberculosis. *Int. J. Mycobacteriol.* **4**, 1–6 (2015).
- P. J. Brennan, H. Nikaido, The envelope of mycobacteria. *Annu. Rev. Biochem.* **64**, 29–63 (1995).
- H. Bloch, Studies on the virulence of tubercle bacilli. *J. Exp. Med.* **97**, 1–16 (1953).
- K. J. Welsh, R. L. Hunter, J. K. Actor, Trehalose 6,6'-dimycolate—A coat to regulate tuberculosis immunopathogenesis. *Tuberculosis* **93**, S3–S9 (2013).
- K. M. Backus, H. I. Boshoff, C. S. Barry, O. Boutureira, M. K. Patel, F. D'Hooge, S. S. Lee, L. E. Via, K. Tahlan, C. E. Barry III, B. G. Davis, Uptake of unnatural trehalose analogs as a reporter for *Mycobacterium tuberculosis*. *Nat. Chem. Biol.* **7**, 228–235 (2011).
- S. R. Rundell, Z. L. Wagar, L. M. Meints, C. D. Olson, M. K. O'Neill, B. F. Piliagian, A. W. Poston, R. J. Hood, P. J. Woodruff, B. M. Swarts, Deoxyfluoro-d-trehalose (FDTre) analogues as potential PET probes for imaging mycobacterial infection. *Org. Biomol. Chem.* **14**, 8598–8609 (2016).
- B. M. Swarts, C. M. Holsclaw, J. C. Jewett, M. Alber, D. M. Fox, M. S. Siegrist, J. A. Leary, R. Kalscheuer, C. R. Bertozzi, Probing the mycobacterial trehalome with bioorthogonal chemistry. *J. Am. Chem. Soc.* **134**, 16123–16126 (2012).
- H. N. Foley, J. A. Stewart, H. W. Kavunja, S. R. Rundell, B. M. Swarts, Bioorthogonal chemical reporters for selective in situ probing of mycomembrane components in mycobacteria. *Angew. Chem. Int. Ed.* **55**, 2053–2057 (2016).
- F. P. Rodríguez-Rivera, X. Zhou, J. A. Theriot, C. R. Bertozzi, Visualization of mycobacterial membrane dynamics in live cells. *J. Am. Chem. Soc.* **139**, 3488–3495 (2017).
- C. R. Barry, Exploiting the biology of trehalose to develop novel imaging probes for tuberculosis, paper presented at the 2016 Annual Meeting for Experimental Biology, San Diego, CA, 6 April 2016.
- J. T. Belisle, V. D. Vissa, T. Sievert, K. Takayama, P. J. Brennan, G. S. Besra, Role of the major antigen of *Mycobacterium tuberculosis* in cell wall biogenesis. *Science* **276**, 1420–1422 (1997).
- J. M. Beck, B. Young, G. B. Huffnagle, The microbiome of the lung. *Transl. Res.* **160**, 258–266 (2012).
- B.-Y. Hong, N. P. Maulén, A. J. Adams, H. Granados, M. E. Balcells, J. Cervantes, Microbiome changes during tuberculosis and antituberculous therapy. *Clin. Microbiol. Rev.* **29**, 915–926 (2016).
- G. Loving, B. Imperiali, A versatile amino acid analogue of the solvatochromic fluorophore 4-*N,N*-dimethylamino-1,8-naphthalimide: A powerful tool for the study of dynamic protein interactions. *J. Am. Chem. Soc.* **130**, 13630–13638 (2008).
- G. Loving, B. Imperiali, Thiol-reactive derivatives of the solvatochromic 4-*N,N*-dimethylamino-1,8-naphthalimide fluorophore: A highly sensitive toolset for the detection of biomolecular interactions. *Bioconjug. Chem.* **20**, 2133–2141 (2009).
- B. N. Goguen, G. S. Loving, B. Imperiali, Development of a fluorogenic sensor for activated Cdc42. *Bioorg. Med. Chem. Lett.* **21**, 5058–5061 (2011).
- E. C. Hett, E. J. Rubin, Bacterial growth and cell division: A mycobacterial perspective. *Microbiol. Mol. Biol. Rev.* **72**, 126–156 (2008).
- J. D. Carroll, I. Pastuszak, V. K. Edavana, T. Y. Pan, A. D. Elbein, A novel trehalase from *Mycobacterium smegmatis*—Purification, properties, requirements. *FEBS J.* **274**, 1701–1714 (2007).
- Y.-T. Pan, J. D. Carroll, N. Asano, I. Pastuszak, V. K. Edavana, A. D. Elbein, Trehalose synthase converts glycogen to trehalose. *FEBS J.* **275**, 3408–3420 (2008).
- R. Kalscheuer, B. Weinrick, U. Veeraraghavan, G. S. Besra, W. R. Jacobs Jr., Trehalose-recycling ABC transporter LpqY-SugA-SugB-SugC is essential for virulence of *Mycobacterium tuberculosis*. *Proc. Natl. Acad. Sci. U.S.A.* **107**, 21761–21766 (2010).
- L. Favrot, A. E. Grzegorzewicz, D. H. Lajiness, R. K. Marvin, J. Boucau, D. Isailovic, M. Jackson, D. R. Ronning, Mechanism of inhibition of *Mycobacterium tuberculosis* antigen 85 by ebsele. *Nat. Commun.* **4**, 2748 (2013).
- H. G. Wiker, M. Harboe, The antigen 85 complex: A major secretion product of *Mycobacterium tuberculosis*. *Microbiol. Rev.* **56**, 648–661 (1992).
- G. S. Timmins, V. Deretic, Mechanisms of action of isoniazid. *Mol. Microbiol.* **62**, 1220–1227 (2006).
- C. Hendry, K. Dionne, A. Hedgepeth, K. Carroll, N. Parrish, Evaluation of a rapid fluorescent staining method for detection of mycobacteria in clinical specimens. *J. Clin. Microbiol.* **47**, 1206–1208 (2009).
- H. X. Xie, J. Mire, Y. Kong, M. H. Chang, H. A. Hassaounah, C. N. Thornton, J. C. Sacchetti, J. D. Cirillo, J. Rao, Rapid point-of-care detection of the tuberculosis pathogen using a BlaC-specific fluorogenic probe. *Nat. Chem.* **4**, 802–809 (2012).
- Y. Cheng, H. Xie, P. Sule, H. Hassaounah, E. A. Graviss, Y. Kong, J. D. Cirillo, J. Rao, Fluorogenic probes with substitutions at the 2 and 7 positions of cephalosporin are highly BlaC-specific for rapid *Mycobacterium tuberculosis* detection. *Angew. Chem. Int. Ed. Engl.* **53**, 9360–9364 (2014).
- S. V. Kik, C. M. Denking, P. Chedore, M. Pai, Replacing smear microscopy for the diagnosis of tuberculosis: What is the market potential? *Eur. Respir. J.* **43**, 1793–1796 (2014).
- S. Datta, J. M. Sherman, M. A. Bravard, T. Valencia, R. H. Gilman, C. A. Evans, Clinical evaluation of tuberculosis viability microscopy for assessing treatment response. *Clin. Infect. Dis.* **60**, 1186–1195 (2014).
- J. P. Diaper, C. Edwards, The use of fluorogenic esters to detect viable bacteria by flow cytometry. *J. Appl. Bacteriol.* **77**, 221–228 (1994).
- C. N. Jacobsen, J. Rasmussen, M. Jakobsen, Viability staining and flow cytometric detection of *Listeria monocytogenes*. *J. Microbiol. Methods* **28**, 35–43 (1997).
- D. Hoefel, W. L. Grooby, P. T. Monis, S. Andrews, C. P. Saint, A comparative study of carboxyfluorescein diacetate and carboxyfluorescein diacetate succinimidyl ester as indicators of bacterial activity. *J. Microbiol. Methods* **52**, 379–388 (2003).
- W. Boos, U. Ehmann, H. Forkl, W. Klein, M. Rimmle, P. Postma, Trehalose transport and metabolism in *Escherichia coli*. *J. Bacteriol.* **172**, 3450–3461 (1990).
- T. C. Ells, L. Truelstrup Hansel, Increased thermal and osmotic stress resistance in *Listeria monocytogenes* 568 grown in the presence of trehalose due to inactivation of the phosphotrehalase-encoding gene *treA*. *Appl. Environ. Microbiol.* **77**, 6841–6851 (2011).
- World Health Organization (WHO), "Systematic screening for active tuberculosis: Principles and recommendations" (WHO Press, 2013); http://apps.who.int/iris/bitstream/10665/84971/1/9789241548601_eng.pdf.
- P. Jain, T. Hsu, M. Arai, K. Biermann, D. S. Thaler, A. Nguyen, P. A. González, J. M. Tufariello, J. Kriakov, B. Chen, M. H. Larsen, W. R. Jacobs Jr., Specialized transduction designed for precise high-throughput unmarked deletions in *Mycobacterium tuberculosis*. *MBio* **5**, e01245–e14 (2014).

Acknowledgments: We thank F. M. Tomlin, S. G. L. Keyser, D. R. Spicariach, D. M. Fox, A. Mclvor, and N. Narrandes for the technical assistance; P. Robinson, C. J. Cambier, and M. Chengalroyen for the helpful discussions; and A. Iavarone [QB3/Chemistry Mass Spectrometry Facility, University of California (UC), Berkeley] for the assistance with mass spectrometry. Flow cytometry was performed in the shared FACS facility at Stanford University on equipment obtained with NIH S10 Shared Instrument grant (S10RR027431-01). **Funding:** M.K. was supported by Stanford University's Diversifying Academia, Recruiting Excellence Fellowship, and the NIH Predoctoral Fellowship F31AI129359. F.P.R.-R. was supported by a Ford Foundation Predoctoral Fellowship and UC Berkeley Chancellor's Fellowship. Data collection was performed on a BD LSR II.UV instrument in the Shared FACS Facility at Stanford University supported by the NIH S10 Shared Instrument grant (S10RR027431-01). R.K. and M.R.B.S. thank the Jurgen Manchot Foundation for the financial support. C.S.E. received a Career Development Award from the South African Medical Research Council. B.D.K. received an International Early Career Scientist Award from the Howard Hughes Medical Institute (HHMI).

Sputum collection and analysis were supported by grants from the South African National Research Foundation (to B.D.K. and C.S.E.), the Centre for the AIDS Programme of Research in South Africa (to C.S.E.), and the Bill and Melinda Gates Foundation (accelerator grant OPP1100182). This research was supported by the Bill and Melinda Gates Foundation (OPP115061) and NIH (AI051622) grants (to C.R.B.). **Author contributions:** P.S., M.K., and C.R.B. designed and led the study. P.S. performed the synthesis and nuclear magnetic resonance analysis. M.K. performed most of the microscopy and flow cytometry experiments. F.P.R.-R. performed the lipid extraction, TLC analysis, and subsequent tandem mass spectrometry analysis. M.R.B.S. generated the MSMEG_6396-99 mutant strain, and M.R.B.S. and R.K. analyzed these data. W.V.T. generated the bacterial tblastn search data. B.C. supported M.K. for the drug treatment of Msmeg experiments. N.M. assisted with the recruitment of TB patients and provision of the sputum samples. J.S.P. and C.S.E. processed the sputum samples and performed DMN-Tre labeling and image analysis of Mtb. B.D.K. led the patient recruitment, patient sputum sample testing, and data analysis. M.K. and C.R.B. analyzed all of the data. M.K., P.S., and C.R.B. wrote and edited the manuscript, which was approved by all authors.

Competing interests: M.K., P.S., and C.R.B. are inventors on U.S. patent application PCT/

US2017/044760 submitted by Stanford University that covers "Methods for detecting mycobacteria with solvatochromic dye conjugates." All other authors declare that they have no competing interests. **Data and materials availability:** Materials are available and will be provided under the material transfer policies of Stanford University and HHMI. These requests should be directed to the corresponding author. Requests for the option to license the technology can be addressed to the Stanford University Office of Technology Licensing.

Submitted 19 December 2016

Accepted 6 February 2018

Published 28 February 2018

10.1126/scitranslmed.aam6310

Citation: M. Kamariza, P. Shieh, C. S. Ealand, J. S. Peters, B. Chu, F. P. Rodriguez-Rivera, M. R. Babu Sait, W. V. Treuren, N. Martinson, R. Kalscheuer, B. D. Kana, C. R. Bertozzi, Rapid detection of *Mycobacterium tuberculosis* in sputum with a solvatochromic trehalose probe. *Sci. Transl. Med.* **10**, eaam6310 (2018).

Rapid detection of *Mycobacterium tuberculosis* in sputum with a solvatochromic trehalose probe

Mireille Kamariza, Peyton Shieh, Christopher S. Ealand, Julian S. Peters, Brian Chu, Frances P. Rodriguez-Rivera, Mohammed R. Babu Sait, William V. Treuren, Neil Martinson, Rainer Kalscheuer, Bavesh D. Kana and Carolyn R. Bertozzi

Sci Transl Med **10**, eaam6310.
DOI: 10.1126/scitranslmed.aam6310

A trehalose tool for tuberculosis

Tuberculosis (TB) is the leading infectious killer worldwide. The prevalence of drug- and multidrug-resistant *Mycobacterium tuberculosis* necessitates more rapid and specific diagnostics. Kamariza *et al.* designed a color-changing dye based on trehalose, a sugar that makes up the outer membrane of *M. tuberculosis*. The dye stained live bacteria within minutes, emitting fluorescence upon incorporation into the hydrophobic mycobacterial membrane. Heat-inactivated bacteria did not fluoresce, and drug-treated bacteria emitted reduced fluorescence. Fluorescence intensity was similar between trehalose analog- and Auramine O-stained human sputum samples from patients with TB. This trehalose-based dye does not require sample washing and emits minimal background fluorescence, which could make it particularly useful for the rapid detection of metabolically active *M. tuberculosis* in resource-limited environments.

ARTICLE TOOLS <http://stm.sciencemag.org/content/10/430/eaam6310>

SUPPLEMENTARY MATERIALS <http://stm.sciencemag.org/content/suppl/2018/02/26/10.430.eaam6310.DC1>

RELATED CONTENT
<http://stm.sciencemag.org/content/scitransmed/9/420/eaal2807.full>
<http://stm.sciencemag.org/content/scitransmed/8/329/329ps7.full>
<http://stm.sciencemag.org/content/scitransmed/7/269/269ra3.full>
<http://stm.sciencemag.org/content/scitransmed/5/214/214ra168.full>
<http://stm.sciencemag.org/content/scitransmed/6/263/263ra159.full>
<http://stm.sciencemag.org/content/scitransmed/10/438/eaal1803.full>
<http://stm.sciencemag.org/content/scitransmed/10/454/eaar4470.full>
<http://stm.sciencemag.org/content/scitransmed/10/470/eaau0965.full>
<http://stm.sciencemag.org/content/scitransmed/11/475/eaat2702.full>
<http://science.sciencemag.org/content/sci/363/6426/457.full>
<http://science.sciencemag.org/content/sci/363/6426/eaau8959.full>
<http://stm.sciencemag.org/content/scitransmed/11/515/eaaw8287.full>
<http://science.sciencemag.org/content/sci/367/6482/1147.full>

REFERENCES This article cites 40 articles, 11 of which you can access for free
<http://stm.sciencemag.org/content/10/430/eaam6310#BIBL>

Use of this article is subject to the [Terms of Service](#)

Science Translational Medicine (ISSN 1946-6242) is published by the American Association for the Advancement of Science, 1200 New York Avenue NW, Washington, DC 20005. The title *Science Translational Medicine* is a registered trademark of AAAS.

Copyright © 2018 The Authors, some rights reserved; exclusive licensee American Association for the Advancement of Science. No claim to original U.S. Government Works

PERMISSIONS

<http://www.sciencemag.org/help/reprints-and-permissions>

Use of this article is subject to the [Terms of Service](#)

Science Translational Medicine (ISSN 1946-6242) is published by the American Association for the Advancement of Science, 1200 New York Avenue NW, Washington, DC 20005. The title *Science Translational Medicine* is a registered trademark of AAAS.

Copyright © 2018 The Authors, some rights reserved; exclusive licensee American Association for the Advancement of Science. No claim to original U.S. Government Works